

1 **MULTISCALE DIFFERENTIAL RICCATI EQUATIONS FOR**
2 **LINEAR QUADRATIC REGULATOR PROBLEMS***

3 AXEL MÅLQVIST[†], ANNA PERSSON[†], AND TONY STILLFJORD[†]

4 **Abstract.** We consider approximations to the solutions of differential Riccati equations in the
5 context of linear quadratic regulator problems, where the state equation is governed by a multiscale
6 operator. Similarly to elliptic and parabolic problems, standard finite element discretizations perform
7 poorly in this setting unless the grid resolves the fine-scale features of the problem. This results in
8 unfeasible amounts of computation and high memory requirements. In this paper, we demonstrate
9 how the localized orthogonal decomposition method may be used to acquire accurate results also
10 for coarse discretizations, at the low cost of solving a series of small, localized elliptic problems.
11 We prove second-order convergence (except for a logarithmic factor) in the L^2 operator norm, and
12 first-order convergence in the corresponding energy norm. These results are both independent of
13 the multiscale variations in the state equation. In addition, we provide a detailed derivation of the
14 fully discrete matrix-valued equations, and show how they can be handled in a low-rank setting for
15 large-scale computations. In connection to this, we also show how to efficiently compute the relevant
16 operator-norm errors. Finally, our theoretical results are validated by several numerical experiments.

17 **Key words.** Multiscale, localized orthogonal decomposition, finite elements, linear quadratic
18 regulator problems, differential Riccati equations

19 **AMS subject classifications.** 49N10, 65N12, 65N30, 93C20

20 **1. Introduction.** In a linear quadratic regulator (LQR) problem, the state x is
21 a model of a system whose evolution can be influenced through the input u . The goal
22 is to drive certain measurable quantities of the system, the output y , to a given target
23 which is typically zero. The relations between x , u and y are given by the state and
24 output equations

25 (1) $\dot{x} = \mathcal{A}x + \mathcal{B}u, \quad x(0) = x_0,$

26 (2) $y = \mathcal{C}x,$

28 where \mathcal{A} , \mathcal{B} and \mathcal{C} are given operators. The optimal input function u^* is found by
29 minimizing the cost functional

30
$$J(u) = \int_0^T (y, y) + (\mathcal{R}u, u) dt,$$

31 where R is a given weighting factor. It can be shown (see e.g. [1, 12]) that u^* is given
32 in feedback form as $u^*(t) = -\mathcal{R}^{-1}\mathcal{B}^*X(T-t)x(t)$, where X is the solution to an
33 operator-valued differential Riccati equation (DRE):

34 (3) $\dot{X}(t) = \mathcal{A}^*X(t) + X(t)\mathcal{A} + \mathcal{C}^*\mathcal{C} - X(t)\mathcal{B}\mathcal{R}^{-1}\mathcal{B}^*X(t),$
35 $X(0) = 0.$

36 In the case of a nonzero output target, one additional differential equation for the
37 evolution of u^* has to be solved.

*Submitted to the editors 2017-06-13.

Funding: This work was supported by the Swedish Research Council under grant no. 2015-04964.

[†]Mathematical Sciences, Chalmers University of Technology and the University of Gothenburg (axel@chalmers.se, peanna@chalmers.se, tony.stillfjord@gu.se.)

38 In this paper, we consider the case when the operator \mathcal{A} exhibits multiscale be-
 39 haviour. This e.g. occurs in the modeling of composite materials and flows in porous
 40 media. Numerically approximating the solutions to elliptic or parabolic equations
 41 given by such operators in the usual way is difficult, because a very fine discretiza-
 42 tion is necessary to resolve the fine-scale structure. These difficulties are exacerbated
 43 when considering DREs such as (3), as their solution essentially requires solving many
 44 parabolic equations.

45 A by now well established method for multiscale elliptic and parabolic problems
 46 is the localized orthogonal decomposition (LOD) [15, 10]. It is a modification of the
 47 finite element method (FEM), which incorporates some of the fine-scale structure into
 48 a coarse discretization by precomputing a series of localized fine-scale problems. Due
 49 to the localization, these are much cheaper to evaluate than the full fine-scale problem
 50 and may additionally be solved in parallel.

51 We note that finite elements were introduced for the approximation of optimal
 52 control problems already in the 1970's, see e.g. [16, 5, 9, 22], and the field has grown
 53 much in several different directions since then. When diffusion problems have been
 54 considered, the focus has typically been on constant or slowly varying diffusion. Re-
 55 cently, however, also optimal control problems of multiscale type have been considered
 56 in e.g. [6, 7, 13]. None of these consider the LOD approach, instead preferring ho-
 57 mogenization or asymptotic expansions. Additionally, a common assumption is that
 58 the multiscale features are periodic, which is frequently not the case in applications.

59 The focus in this paper is on the approximation of DREs such as (3). In contrast
 60 to the forward-adjoint approach, which solves a specific optimal control problem, the
 61 DRE provides the feedback laws for all problems defined by the operators $\mathcal{A}, \mathcal{B}, \mathcal{C}$.
 62 While more expensive to solve, it can be precomputed and reused in many different
 63 situations. We refer to [4, 12] for an overview of Riccati theory, with the latter
 64 reference treating very general problems.

65 Our main result is that LOD-approximations to the solution of (3) with a mesh
 66 size H converge with order $H^2 \log(H^{-1})$ in the L^2 operator norm to a given accurate
 67 fine-scale FEM approximation. The convergence in the corresponding operator energy
 68 norm is shown to be of order H . We note that $H^2 \log(H^{-1})$ -convergence of FEM
 69 approximations to the exact solution of (3) has previously been shown in [11], and
 70 similar results for algebraic Riccati equations can be found in [12]. (See also [17, 3] for
 71 convergence results without orders in related settings.) However, the error constants
 72 in these results depend on the multiscale variations of \mathcal{A} , and thus such convergence
 73 is not observed in practice. This is not the case for our present results.

74 For practical computations, also a temporal discretization is necessary; for this
 75 we consider a low-rank splitting scheme as introduced in [18]. Such methods decom-
 76 pose the DRE into its affine and nonlinear parts and approximate these separately,
 77 thereby greatly reducing the computational cost. The affine problem requires the
 78 approximation of several parabolic equations involving \mathcal{A} in each time step. As the
 79 computational efficiency gain for LOD increases with the number of times the mod-
 80 ified basis may be reused, splitting schemes are thus particularly well suited to be
 81 combined with the LOD method.

82 We demonstrate how to transform the FEM and LOD discretizations into matrix-
 83 valued equations, and how to implement the fully discrete methods. Even if LOD
 84 reduces the need for very fine discretizations, large 2D or 3D-problems may still yield
 85 large matrices. We therefore consider the low-rank approach, which greatly reduces
 86 the necessary amount of computations. As a side effect, this also allows us to compute
 87 errors in the operator norms very efficiently.

88 A brief outline of the paper is as follows: We formalize the setting and our basic
 89 assumptions in [section 2](#), and define the different spatial discretizations in [section 3](#).
 90 Convergence of the LOD approximations with the appropriate order is then shown
 91 in [section 4](#). The matrix-valued formulations of the discretized DREs and related
 92 questions are discussed in [section 5](#), while [section 6](#) is devoted to the temporal dis-
 93 cretization and low-rank setting. Finally, we present several numerical experiments
 94 and their results in [section 7](#).

95 **2. Setting.** Let $\Omega \in \mathbb{R}^d$, $d \leq 3$, be a bounded polygonal/polyhedral domain.
 96 We consider the separable Hilbert spaces $L^2(\Omega)$, $V = H_0^1(\Omega)$, U and Z , where $L^2(\Omega)$
 97 corresponds to the state space, U is the control space and Z is the observation space.
 98 In the following, the specification of Ω will be omitted. We write (\cdot, \cdot) and $\|\cdot\|$ for
 99 the inner product and norm on L^2 , and denote the corresponding quantities on V ,
 100 U and Z by subscripts. To define the state evolution operator \mathcal{A} , we assume that
 101 the inner product $a(u, v) = \int \kappa \nabla u \cdot \nabla v$ on $V \times V$ is given, with assumptions on
 102 κ given below. Then $\mathcal{A}: L^2 \supset \mathcal{D}(\mathcal{A}) \rightarrow L^2$ is defined by $(\mathcal{A}u, v) = -a(u, v)$ and
 103 $\mathcal{D}(\mathcal{A}) = \{u \in V \mid \mathcal{A}u \in L^2\}$.

104 Further, let the input operator $\mathcal{B}: U \rightarrow L^2$ and the output operator $\mathcal{C}: L^2 \rightarrow Z$
 105 be given. We also consider the output weighting operator $\mathcal{R}: U \rightarrow U$, which could
 106 be included in \mathcal{B} but is typically not. By $*$, we denote Hilbert-adjoint operators with
 107 respect to L^2 , so that e.g. $\mathcal{B}^*: L^2 \rightarrow U$ satisfies $(\mathcal{B}x, y) = (x, \mathcal{B}^*y)$ for all $x \in U$ and
 108 $y \in L^2$. Finally, we denote the linear bounded operators from one generic Hilbert
 109 space, Y , to another, W , by $\mathcal{L}(Y, W)$. When $W = Y$, we abbreviate $\mathcal{L}(Y) = \mathcal{L}(Y, Y)$.
 110 In this notation, the weak form of [\(3\)](#) is to find $X \in \mathcal{L}(L^2)$ satisfying

$$111 \quad (4) \quad \left(\dot{X}x, y \right) = (Xx, \mathcal{A}y) + (Xy, \mathcal{A}x) + (\mathcal{C}x, \mathcal{C}y)_Z - (\mathcal{R}^{-1} \mathcal{B}^* Xx, \mathcal{B}^* Xy)_U,$$

112 for all $x, y \in \mathcal{D}(\mathcal{A})$.

113 **ASSUMPTION 2.1.** *The diffusion coefficient $\kappa \in L^\infty(\mathbb{R}^{d \times d})$ is symmetric and sat-*
 114 *isfies*

$$115 \quad 0 < \alpha := \operatorname{ess\,inf}_{x \in \Omega} \inf_{v \in \mathbb{R}^d \setminus \{0\}} \frac{\kappa(x)v \cdot v}{v \cdot v}$$

$$116 \quad \infty > \beta := \operatorname{ess\,sup}_{x \in \Omega} \sup_{v \in \mathbb{R}^d \setminus \{0\}} \frac{\kappa(x)v \cdot v}{v \cdot v}.$$

117

118 *In addition, $\mathcal{B} \in \mathcal{L}(U, L^2)$, $\mathcal{C} \in \mathcal{L}(L^2, Z)$ and $\mathcal{R} \in \mathcal{L}(U)$ is invertible with $\mathcal{R}^{-1} \in \mathcal{L}(U)$.*

119 The first part of [Assumption 2.1](#) shows that a is a bounded and coercive bilinear
 120 form, which means that \mathcal{A} is the generator of an analytic semigroup $e^{t\mathcal{A}}: L^2 \rightarrow L^2$,
 121 see e.g. [\[20, Theorem 3.6.1\]](#). In conjunction with the boundedness assumptions on \mathcal{B} , \mathcal{C}
 122 and \mathcal{R} , this guarantees the existence and uniqueness of a solution to [\(4\)](#). In fact, there
 123 is even a classical solution to [\(3\)](#) [\[4, Part IV, Ch. 3\]](#), which means that the $\mathcal{A}^*X + X\mathcal{A}$
 124 term can be extended to an operator in $\mathcal{L}(L^2)$. As a consequence, Equation [\(4\)](#) holds
 125 also for $x, y \in L^2$. We note that these conclusions are valid also under various weaker
 126 forms of [Assumption 2.1](#), which additionally permit the treatment of boundary control
 127 and observation. Since these are not critical to the aim of this article, we simply refer
 128 to e.g. [\[12\]](#).

129 **3. Spatial discretization.** We first introduce the FEM approximation of [\(4\)](#).
 130 To this end, we let \mathcal{T}_h be a triangulation of Ω with meshwidth h and N_h internal

131 nodes. The subspace $V_h \subset V$ denotes the space of continuous and piecewise affine
 132 functions on \mathcal{T}_h , and we denote the corresponding nodal basis functions by $\{\varphi_i^h\}_{i=1}^{N_h}$.
 133 This discretization is referred to as the fine, or sometimes also reference, mesh, see
 134 further [subsection 3.1](#) below.

135 We also consider a coarse discretization space $V_H \subset V_h$ for $H > h$, with the cor-
 136 responding family of triangulations $\{\mathcal{T}_H\}_{H>h}$, which is assumed to be quasi-uniform.
 137 For these triangulations, we let B_K be the largest ball contained in K and denote by
 138 $\gamma > 0$ the shape regularity of the mesh, defined by

$$139 \quad \gamma := \max \gamma_K, \quad \gamma_K := \frac{\text{diam } B_K}{\text{diam } K}, \quad \forall K \in \mathcal{T}_H, \quad H > h.$$

141 Furthermore, we let $\text{Id}_H^h: V_H \rightarrow V_h$ denote the identity operator between these spaces,
 142 i.e. $\text{Id}_H^h u = u$ for all $u \in V_H$. Similarly, $\text{Id}_h: V_h \rightarrow L^2$ is the identity operator mapping
 143 into L^2 and Id_h^* is the L^2 -orthogonal projection of L^2 onto V_h .

144 The semi-discretized weak form of (3) is defined by

$$145 \quad (5) \quad (\dot{X}_h x, y) = (X_h x, \mathcal{A}_h y) + (X_h y, \mathcal{A}_h x) + (\mathcal{C}_h x, \mathcal{C}_h y)_Z - (\mathcal{R}^{-1} \mathcal{B}_h^* X_h x, \mathcal{B}_h^* X_h y)_U.$$

146 for all $x, y \in V_h$ and with $X_h: V_h \rightarrow V_h$ satisfying $X_h(0) = \text{Id}_h^* X(0) \text{Id}_h$. Here, the
 147 operators $\mathcal{A}_h: V_h \rightarrow V_h$, $\mathcal{B}_h: U \rightarrow V_h$ and $\mathcal{C}_h: V_h \rightarrow Z$ satisfy

$$148 \quad (\mathcal{A}_h x, y) = (\mathcal{A} x, y), \quad (\mathcal{B}_h u, y) = (\mathcal{B} u, y) \quad \text{and} \quad (\mathcal{C}_h x, z) = (\mathcal{C} x, z)$$

149 for all $x, y \in V_h$, $u \in U$ and $z \in Z$. We note that X can be proven to be self-adjoint,
 150 so we additionally require that X_h is self-adjoint.

151 For the coarse discretization, we have the same equation but with H instead of
 152 h . We observe that the coarse and fine operators are related in the following way:

$$153 \quad (6) \quad \mathcal{A}_H = (\text{Id}_H^h)^* \mathcal{A}_h \text{Id}_H^h, \quad \mathcal{B}_H = (\text{Id}_H^h)^* \mathcal{B}_h \quad \text{and} \quad \mathcal{C}_H = \mathcal{C}_h \text{Id}_H^h,$$

154 and that the natural extension of X_H to a map on V_h is given by $\text{Id}_H^h X_H (\text{Id}_H^h)^*$.
 155 Here, $(\text{Id}_H^h)^*$ is the L^2 -orthogonal projection of V_h onto V_H .

156 **3.1. Localized orthogonal decomposition.** If κ is varying on a small scale
 157 of size $\epsilon > 0$, then the classical FEM approximation of a parabolic problem $\dot{x} =$
 158 $\mathcal{A}x + f$ may yield poor results, unless h is sufficiently small to resolve the fine-scale
 159 variations. That is, we typically do not observe $O(h^2)$ -convergence until $h < \epsilon$, which
 160 requires infeasible amounts of computation. The same behaviour occurs for the X_h -
 161 discretizations of (4).

162 To this end, we assume that h is sufficiently small so that X_h is a good approxima-
 163 tion of X . That is, $h < \epsilon$, and we refer to X_h as the reference solution. The aim is now
 164 to approximate X_h by using a multiscale space $V_{\text{ms}} \subset V_h$ of the same dimension as
 165 the coarse space V_H . To obtain such a space, we use the localized orthogonal decom-
 166 position (LOD) method introduced in [15], which incorporates fine-scale information
 167 in the coarse-scale space. The construction involves the solution of several fine-scale,
 168 but localized and parallelizable, problems. We briefly summarize the procedure here
 169 and refer to [15, 10], for the details.

170 To define the multiscale space V_{ms} , we first introduce an interpolation operator
 171 $I_H: V_h \rightarrow V_H$ that fulfills

$$172 \quad 173 \quad H^{-1} \|v - I_H v\|_{L^2(K)} + \|\nabla I_H v\|_{L^2(K)} \leq C \|\nabla v\|_{L^2(\omega_K)}, \quad \forall v \in V_h,$$

174 for all triangles $K \in \mathcal{T}_H$, where $\omega_K := \cup\{\hat{K} \in \mathcal{T}_H : \hat{K} \cap K \neq \emptyset\}$. In this paper we use
 175 the weighted Clément interpolant as in [15]. Let V_f denote the kernel of I_H ,

$$176 \quad V_f := \ker I_H = \{v \in V_h : I_H v = 0\},$$

178 and note that V_h can be decomposed as $V_h = V_H \oplus V_f$, meaning that every $v_h \in V_h$
 179 can be written as $v_h = v_H + v_f$ with $v_H \in V_H, v_f \in V_f$. We now introduce the (global)
 180 correction operator $\hat{Q}_h : V_H \rightarrow V_f$ by

$$181 \quad a(\hat{Q}_h v, w) = a(v, w), \quad \forall w \in V_f,$$

183 and define the (global) multiscale space as $\hat{V}_{\text{ms}} := \hat{R}_h V_H = V_H - \hat{Q}_h V_H$, with $\hat{R}_h :=$
 184 $\text{Id}_H^h - \hat{Q}_h$. This leads to the decomposition $V_h = \hat{V}_{\text{ms}} \oplus V_f$ with the orthogonality
 185 $a(\hat{v}_{\text{ms}}, v_f) = 0$, $\hat{v}_{\text{ms}} \in \hat{V}_{\text{ms}}, v_f \in V_f$. Note that \hat{Q}_h is the orthogonal projection onto V_f
 186 with respect to the inner product $a(\cdot, \cdot)$, i.e. the Ritz projection onto V_f , and \hat{V}_{ms} is
 187 the orthogonal complement to V_f . From the construction it follows that $\dim \hat{V}_{\text{ms}} =$
 188 $\dim V_H$. Indeed, a basis for \hat{V}_{ms} is given by $\{\varphi_i^H - \hat{Q}_h \varphi_i^H : i = 1, \dots, N_H\}$.

189 In general, the corrections $\hat{Q}_h \varphi_i^H$ have global support and are expensive to com-
 190 pute, since they are posed in the entire fine scale space $V_f \subseteq V_h$. To overcome this,
 191 it is observed that the corrections have exponential decay away from the i :th node of
 192 \mathcal{T}_H (see [15, 10]), which motivates a truncation of the corrections. For this purpose,
 193 we define patches $\omega_k(K)$ of size k around each $K \in \mathcal{T}_H$ by the following:

$$194 \quad \omega_0(K) := \text{int } K,$$

$$195 \quad \omega_k(K) := \text{int} \left(\cup \{ \hat{K} \in \mathcal{T}_H : \hat{K} \cap \overline{\omega_{k-1}(K)} \neq \emptyset \} \right), \quad k = 1, 2, \dots$$

197 Further, we define $V_f^K := \{v \in V_f : v(z) = 0 \text{ on } \overline{\Omega} \setminus \omega_k(K)\}$ to be the restriction
 198 of V_f to the patch $\omega_k(K)$. For brevity, we do not include the dependence on k in
 199 the notation. Now note that the correction operator \hat{Q}_h can be written as the sum
 200 $\hat{Q}_h = \sum_{K \in \mathcal{T}_H} \hat{Q}_h^K$, where

$$201 \quad a(\hat{Q}_h^K v, w) = \int_K \kappa \nabla v \cdot \nabla w, \quad \forall w \in V_f, v \in V_H, K \in \mathcal{T}_H.$$

203 We can now localize these computations by replacing V_f with V_f^K . Define $Q_h^K : V_H \rightarrow$
 204 V_f^K such that

$$205 \quad a(Q_h^K v, w) = \int_K \kappa \nabla v \cdot \nabla w, \quad \forall w \in V_f^K, v \in V_H, K \in \mathcal{T}_H.$$

207 Finally, we can define a local operator $Q_h := \sum_{K \in \mathcal{T}_H} Q_h^K$ and a localized space
 208 $V_{\text{ms}} := R_h V_H = V_H - Q_h V_{\text{ms}}$, with $R_h := \text{Id}_H^h - Q_h$.

209 The approximation properties (and the required computational effort) of the space
 210 V_{ms} depends on the choice of k . In [10] it is proven that convergence of order H^2 is
 211 obtained if k is chosen proportional to $\log H^{-1}$. In this paper we therefore assume
 212 that $k \sim \log H^{-1}$ to avoid explicitly stating the dependence on k .

213 To define an LOD-approximation to the solution X_h in (5), we additionally need
 214 to introduce the identity operator $\text{Id}_{\text{ms}}^h : V_{\text{ms}} \rightarrow V_h$, $\text{Id}_{\text{ms}}^h u = u$. Its L^2 -adjoint is
 215 the L^2 -orthogonal projection of V_h onto V_{ms} . Replacing the space V_h with V_{ms} then
 216 results in the problem to find $X_h^{\text{ms}} : V_{\text{ms}} \rightarrow V_{\text{ms}}$ satisfying

$$217 \quad (7) \quad \begin{aligned} \left(\dot{X}_h^{\text{ms}} u, v \right) &= (X_h^{\text{ms}} u, \mathcal{A}_h^{\text{ms}} v) + (X_h^{\text{ms}} v, \mathcal{A}_h^{\text{ms}} u) \\ &\quad + (\mathcal{C}_h^{\text{ms}} u, \mathcal{C}_h^{\text{ms}} v)_Z - (\mathcal{R}^{-1}(\mathcal{B}_h^{\text{ms}})^* X_h^{\text{ms}} u, (\mathcal{B}_h^{\text{ms}})^* X_h^{\text{ms}} v)_U \end{aligned}$$

218 for all $u, v \in V_{\text{ms}}$ and the initial condition $X_h^{\text{ms}}(0) = (\text{Id}_{\text{ms}}^h)^* \text{Id}_h^* X(0) \text{Id}_h \text{Id}_{\text{ms}}^h$. Here,
 219 the operators $\mathcal{A}_h^{\text{ms}}: V_{\text{ms}} \rightarrow V_{\text{ms}}$, $\mathcal{B}_h^{\text{ms}}: U \rightarrow V_{\text{ms}}$ and $\mathcal{C}_h^{\text{ms}}: V_{\text{ms}} \rightarrow Z$ are given by

$$220 \quad (\mathcal{A}_h^{\text{ms}} v, w) = (\mathcal{A} v, w), \quad (\mathcal{B}_h^{\text{ms}} u, w)_U = (\mathcal{B} u, w)_U \quad \text{and} \quad (\mathcal{C}_h^{\text{ms}} v, z)_Z = (\mathcal{C} u, z)_Z$$

222 for all $v, w \in V_{\text{ms}}$, $u \in U$ and $z \in Z$. Similar to (6) we have

$$223 \quad (8) \quad \mathcal{A}_h^{\text{ms}} = (\text{Id}_{\text{ms}}^h)^* \mathcal{A}_h \text{Id}_{\text{ms}}^h, \quad \mathcal{B}_h^{\text{ms}} = (\text{Id}_{\text{ms}}^h)^* \mathcal{B}_h \quad \text{and} \quad \mathcal{C}_h^{\text{ms}} = \mathcal{C}_h \text{Id}_{\text{ms}}^h.$$

224 The natural V_h -extension of X_h^{ms} is given by $\text{Id}_{\text{ms}}^h X_h^{\text{ms}} (\text{Id}_{\text{ms}}^h)^*$, similar to the X_H -case.

225 Since V_{ms} has the same dimension as V_H , there is a lower-dimensional represen-
 226 tative for X_h^{ms} , given by $X_h^{\text{ms}} = R_h X_H^{\text{ms}} R_h^{-1}$. By inserting $u = R_h x$ and $v = R_h y$,
 227 with $x, y \in V_H$, in (7) we see that

$$228 \quad \left(\dot{X}_H^{\text{ms}} x, R_h^* R_h y \right) = (X_H^{\text{ms}} x, R_h^* \mathcal{A}_h R_h y) + (X_H^{\text{ms}} y, R_h^* \mathcal{A}_h R_h x) \\
 229 \quad \quad \quad + (\mathcal{C}_h R_h x, \mathcal{C}_h R_h y)_Z - (\mathcal{R}^{-1} \mathcal{B}_h^* R_h X_H^{\text{ms}} x, \mathcal{B}_h^* R_h X_H^{\text{ms}} y)_U,$$

231 and we consequently define the corrected coarse-scale operators

$$232 \quad \mathcal{A}_H^{\text{ms}} = R_h^* \mathcal{A}_h R_h, \quad \mathcal{B}_H^{\text{ms}} = R_h^* \mathcal{B}_h \quad \text{and} \quad \mathcal{C}_H^{\text{ms}} = \mathcal{C}_h R_h.$$

233 **4. Error analysis.** In the following, C denotes a generic constant which may
 234 take different values at different occasions. It may depend on the problem data and
 235 the size of the domain, but is independent of h and H . Moreover, it does not depend
 236 on the multiscale variations of \mathcal{A} , i.e. any derivatives of κ . We start by gathering
 237 some useful results:

238 **4.1. Preliminaries.** Recall that $\text{Id}_h: V_h \rightarrow L^2$ is the identity mapping, $P_h =$
 239 $\text{Id}_h^*: L^2 \rightarrow V_h$ denotes the L^2 -orthogonal projection onto V_h , and P_{ms} is the L^2 -
 240 orthogonal projection onto V_{ms} . We have $P_{\text{ms}} = (\text{Id}_{\text{ms}}^h)^* P_h$, i.e. we first project onto
 241 V_h and then onto V_{ms} . Straightforward calculations show the following:

242 LEMMA 4.1. *Under Assumption 2.1, it holds that $\text{Id}_h \mathcal{B}_h \in \mathcal{L}(U, L^2)$, $\mathcal{C}_h P_h \in$
 243 $\mathcal{L}(L^2, Z)$ and $S_h := \text{Id}_h \mathcal{B}_h \mathcal{R}^{-1} \mathcal{B}_h^* \text{Id}_h^* \in \mathcal{L}(L^2)$.*

244 Further, let $e^{t\mathcal{A}_h}$ denote the solution operator to the equation $\dot{u} + \mathcal{A}_h u = 0$, i.e. the
 245 semigroup generated by \mathcal{A}_h . Similarly, $e^{t\mathcal{A}_h^{\text{ms}}}$ is the semigroup generated by $\mathcal{A}_h^{\text{ms}}$.
 246 Because \mathcal{A} generates an analytic semigroup on L^2 , these operators are analytic semi-
 247 groups on V_h and V_{ms} , respectively. More specifically, we have

248 LEMMA 4.2. *Under Assumption 2.1, the operators*

$$249 \quad E_h(t) = \text{Id}_h e^{t\mathcal{A}_h} \text{Id}_h^* \quad \text{and} \quad E_{\text{ms}}(t) = \text{Id}_h \text{Id}_{\text{ms}}^h e^{t\mathcal{A}_h^{\text{ms}}} (\text{Id}_{\text{ms}}^h)^* \text{Id}_h^*,$$

250 are both in $\mathcal{L}(L^2)$ for $t \in [0, T]$, with the uniform bounds $\|E_h(t)\|_{\mathcal{L}(L^2)} \leq 1$ and
 251 $\|E_{\text{ms}}(t)\|_{\mathcal{L}(L^2)} \leq 1$.

252 By arguing as in [14], but for the (simpler) semi-discrete case, we have (choosing
 253 $k \sim \log H$)

254 LEMMA 4.3. *For $t \in (0, T]$ it holds that*

$$255 \quad \|E_h(t) - E_{\text{ms}}(t)\|_{\mathcal{L}(L^2)} \leq CH^2 t^{-1}.$$

256 Here, the constant C depends on T , α , β , and γ , but not on the multiscale variations
 257 of \mathcal{A} .

258 *Proof.* We only comment briefly on the proof here. Let $u_h(t) = e^{t\mathcal{A}_h}P_h v$ and
 259 $u_{\text{ms}}(t) = e^{t\mathcal{A}_h^{\text{ms}}}P_{\text{ms}}v$, for $v \in L^2(\Omega)$. By introducing the Ritz projection $R_{\text{ms}}: V_h \rightarrow$
 260 V_{ms} satisfying $a(R_{\text{ms}}v, w) = a(v, w)$ for all $w \in V_{\text{ms}}, v \in V_h$ we get, see [21, Chapter
 261 3] and [14],

$$262 \quad \|u_h - u_{\text{ms}}\| \leq Ct^{-1} \sup_{s \leq t} \left\{ s^2 \|\dot{\rho}\| + s \|\rho\| + \left\| \int_0^s \rho(r) dr \right\| \right\},$$

264 where $\rho := u_h - R_{\text{ms}}u_h$. From the error bounds of R_{ms} in [15], see also [14], we get

$$265 \quad \|u_h - u_{\text{ms}}\| \leq CH^2(s^2 \|\ddot{u}_h(s)\| + s \|\dot{u}_h(s)\| + \|u_h(s)\| + \|v\|).$$

266 The regularity estimates $\|D_t^l u_h(t)\| \leq Ct^{-l} \|v\|$, for $t = 0, 1, 2$, [21, Lemma 2.5],
 267 completes the proof. \square

268 Finally, from Lemma 4.1, we get the existence and uniqueness of solutions X_h and
 269 X_h^{ms} to the discretized DREs (5) and (7), respectively. Let us abbreviate

$$270 \quad \tilde{X}(t) = \text{Id}_h X_h(t) \text{Id}_h^* \quad \text{and} \quad \tilde{Y}(t) = \text{Id}_h \text{Id}_{\text{ms}}^h X_h^{\text{ms}} (\text{Id}_{\text{ms}}^h)^* \text{Id}_h^*.$$

271 Then we have

272 LEMMA 4.4. *There is a constant $C > 0$ which is independent of the multiscale*
 273 *variations of \mathcal{A} but may depend on α and β , such that*

$$274 \quad \|\tilde{X}(t)\|_{\mathcal{L}(L^2)} + \|\tilde{Y}(t)\|_{\mathcal{L}(L^2)} \leq C,$$

275 for $t \in [0, T]$.

276 **4.2. Error analysis.** We are now ready for the main theorem of this paper:

277 THEOREM 4.5. *Suppose that Assumption 2.1 is fulfilled. Then for $t \in (0, T]$ it*
 278 *holds that*

$$279 \quad \|\tilde{X}(t) - \tilde{Y}(t)\|_{\mathcal{L}(L^2)} \leq CH^2(\log(H^{-1}) + t^{-1}).$$

280 Here, the constant C depends on T, α, β, γ , and $\|X(0)\|_{\mathcal{L}(L^2)}$, but not on the multi-
 281 scale variations of \mathcal{A} .

282 *Proof.* We utilize the integral form of (5). If X_h solves (5) then it satisfies

$$283 \quad (9) \quad X_h(t) = e^{t\mathcal{A}_h^*} X_h(0) e^{t\mathcal{A}_h} + \int_0^t e^{(t-s)\mathcal{A}_h^*} \left(\mathcal{C}_h^* \mathcal{C}_h - X_h(s) \mathcal{B}_h \mathcal{R}^{-1} \mathcal{B}_h^* X_h(s) \right) e^{(t-s)\mathcal{A}_h} ds.$$

284 (see e.g. [4, Chapter IV:3, Proposition 2.1]). Recalling that $\text{Id}_h^* \text{Id}_h$ and $(\text{Id}_{\text{ms}}^h)^* \text{Id}_{\text{ms}}^h$
 285 are the identity operators on V_h and V_{ms} , respectively, and using (8) therefore shows
 286 that

$$287 \quad \tilde{X}(t) = E_h(t)^* \tilde{X}(0) E_h(t) + \int_0^t E_h(t-s)^* \left((\mathcal{C}_h P_h)^* \mathcal{C}_h P_h - \tilde{X}(s) S_h \tilde{X}(s) \right) E_h(t-s) ds,$$

288 as well as

$$289 \quad \tilde{Y}(t) = E_{\text{ms}}(t)^* \tilde{X}(0) E_{\text{ms}}(t) + \int_0^t E_{\text{ms}}(t-s)^* \left((\mathcal{C}_h P_h)^* \mathcal{C}_h P_h - \tilde{Y}(s) S_h \tilde{Y}(s) \right) E_{\text{ms}}(t-s) ds. \blacksquare$$

290 (Note the $\tilde{X}(0)$ in the first term, since we suppose $X_h^{\text{ms}}(0) = (\text{Id}_{\text{ms}}^h)^* X_h(0) \text{Id}_{\text{ms}}^h$.)
 291 Subtracting these expressions yields

$$\begin{aligned}
 292 \quad \tilde{X}(t) - \tilde{Y}(t) &= E_h(t)^* \tilde{X}(0) \left(E_h(t) - E_{\text{ms}}(t) \right) + \left(E_h(t) - E_{\text{ms}}(t) \right)^* \tilde{X}(0) E_{\text{ms}}(t) \\
 293 \quad &+ \int_0^t E_h(t-s)^* (\mathcal{C}_h P_h)^* (\mathcal{C}_h P_h) \left(E_h(t-s) - E_{\text{ms}}(t-s) \right) \\
 294 \quad &+ \left(E_h(t-s) - E_{\text{ms}}(t-s) \right)^* (\mathcal{C}_h P_h)^* (\mathcal{C}_h P_h) E_{\text{ms}}(t-s) \\
 295 \quad &+ \left(E_h(t-s) - E_{\text{ms}}(t-s) \right)^* \tilde{X}(s) S_h \tilde{X}(s) E_h(t-s) \\
 296 \quad &+ E_{\text{ms}}(t-s)^* \tilde{X}(s) S_h \tilde{X}(s) \left(E_h(t-s) - E_{\text{ms}}(t-s) \right) \\
 297 \quad &+ E_{\text{ms}}(t-s)^* \left(\tilde{X}(s) - \tilde{Y}(s) \right) S_h \tilde{X}(s) E_{\text{ms}}(t-s) \\
 298 \quad &+ E_{\text{ms}}(t-s)^* \tilde{Y}(s) S_h \left(\tilde{X}(s) - \tilde{Y}(s) \right) E_{\text{ms}}(t-s) \, ds \\
 299 \quad &=: R_1 + R_2 + \int_0^t \sum_{j=3}^8 R_j(s) \, ds, \\
 300
 \end{aligned}$$

301 so that

$$302 \quad \|\tilde{X}(t) - \tilde{Y}(t)\|_{\mathcal{L}(L^2)} \leq \|R_1\|_{\mathcal{L}(L^2)} + \|R_2\|_{\mathcal{L}(L^2)} + \int_0^t \left\| \sum_{j=3}^8 R_j(s) \right\|_{\mathcal{L}(L^2)} \, ds.$$

303 We observe that for all $G: L^2 \rightarrow Y$ (with a generic Hilbert space Y) it holds that
 304 $\|G\|_{\mathcal{L}(L^2, Y)} = \|G^*\|_{\mathcal{L}(Y, L^2)}$. Thus, using [Lemmas 4.2](#) to [4.4](#) we get

$$305 \quad \|R_1\|_{\mathcal{L}(L^2)} = \|R_2\|_{\mathcal{L}(L^2)} \leq CH^2 t^{-1} \|\tilde{X}(0)\|_{\mathcal{L}(L^2)} \leq CH^2 t^{-1},$$

306 Additionally using [Lemma 4.1](#) shows that the last two integrands satisfy

$$\begin{aligned}
 307 \quad \|R_7(s) + R_8(s)\|_{\mathcal{L}(L^2)} &\leq CH^2 \left(\|\tilde{X}(s)\|_{\mathcal{L}(L^2)} + \|\tilde{Y}(s)\|_{\mathcal{L}(L^2)} \right) \|\tilde{X}(s) - \tilde{Y}(s)\|_{\mathcal{L}(L^2)} \\
 308 \quad &\leq CH^2 \|\tilde{X}(s) - \tilde{Y}(s)\|_{\mathcal{L}(L^2)}.
 \end{aligned}$$

310 Due to the singularity at $s = t$ in the bound on $\|E_h(t-s) - E_{\text{ms}}(t-s)\|_{\mathcal{L}(L^2)}$, we
 311 split the integrals of the remaining R_j -terms into two parts. For R_3 , we find

$$\begin{aligned}
 312 \quad \int_0^t \|R_3(s)\|_{\mathcal{L}(L^2)} \, ds &\leq \int_0^{t-H^2} C \|\mathcal{C}_h P_h\|_{\mathcal{L}(L^2)}^2 H^2 (t-s)^{-1} \, ds + \int_{t-H^2}^t 2 \|\mathcal{C}_h P_h\|_{\mathcal{L}(L^2)}^2 \, ds \\
 313 \quad &\leq CH^2 (\log t - 2 \log H) + CH^2 \\
 314 \quad &\leq CH^2 (\log(H^{-1}) + t^{-1}), \\
 315
 \end{aligned}$$

316 where we have used $t \leq T$ for the crude estimate $\log t \leq Ct^{-1}$, since a t^{-1} -term
 317 already appears in the bounds of R_1 and R_2 . The same bound holds for R_4 , and, by
 318 [Lemma 4.1](#) and [Lemma 4.4](#), also for R_5 and R_6 . In conclusion, we thus have \square

$$319 \quad \|\tilde{X}(t) - \tilde{Y}(t)\|_{\mathcal{L}(L^2)} \leq CH^2 (\log(H^{-1}) + t^{-1}) + CH^2 \int_0^t \|\tilde{X}(s) - \tilde{Y}(s)\|_{\mathcal{L}(L^2)} \, ds,$$

320 which by Grönwall's lemma yields the statement of the theorem.

321 *Remark 4.6.* In the common case that $X(0) = 0$, corresponding to the case of no
322 final state penalization, the t^{-1} -singularity disappears.

323 *Remark 4.7.* We note that a bound of the same form has been shown in [11] for
324 the FEM error. However, the error constant then depends on κ , and one does not
325 observe the given convergence order until $H < \epsilon$.

326 Similar to the parabolic case, the error bound becomes less singular near $t = 0$
327 if we measure in the V -norm. To prove this we need the following, slightly stronger,
328 assumptions on the operators (cf. [Assumption 2.1](#)):

329 **ASSUMPTION 4.8.** *In addition to [Assumption 2.1](#), $\mathcal{B} \in \mathcal{L}(U, V)$, $\mathcal{C} \in \mathcal{L}(V, Z)$, and*
330 *$X(0) \in \mathcal{L}(V)$. Moreover, we assume that the mesh \mathcal{T}_h is of a form such that P_h is*
331 *stable in the V -norm.*

332 *Remark 4.9.* In particular, quasi-uniform meshes satisfy [Assumption 4.8](#). We
333 refer to [2] for a discussion on more general permissible meshes.

334 **THEOREM 4.10.** *Suppose that [Assumption 4.8](#) is fulfilled. For $t \in (0, T]$ it holds*
335 *that*

$$336 \quad \|\tilde{X}(t) - \tilde{Y}(t)\|_{\mathcal{L}(V)} \leq CHt^{-1/2}.$$

337 *Here, the constant C depends on T , α , β , γ , and $\|X(0)\|_{\mathcal{L}(V)}$, but not on the multiscale*
338 *variations of \mathcal{A} .*

339 *Proof.* We start by noting that $\|\text{Id}_h\|_{\mathcal{L}(V_h, V)} \leq 1$. Furthermore, since P_h is stable
340 in the V -norm, the following bound holds

$$341 \quad \|P_h\|_{\mathcal{L}(V, V_h)} = \sup_{v \in V} \frac{\|P_h v\|_V}{\|v\|_V} \leq \sup_{v \in V} \frac{C\|v\|_V}{\|v\|_V} \leq C.$$

343 Now, note that if the initial data $v \in V$ then we may instead of [Lemma 4.3](#) prove
344 the following, less singular, error bound

$$345 \quad \|E_h(t) - E_{\text{ms}}(t)\|_{\mathcal{L}(V)} \leq CHt^{-1/2}.$$

347 In addition, parabolic regularity gives the bounds $\|E_h(t)\|_{\mathcal{L}(V)}, \|E_{\text{ms}}(t)\|_{\mathcal{L}(V)} \leq C$.

348 Note that $\|\mathcal{C}_h\|_{\mathcal{L}(V_h, Z)} \leq \|\mathcal{C}\|_{\mathcal{L}(V, Z)}$, so from [Assumption 4.8](#) it follows that

$$349 \quad (10) \quad \begin{aligned} & \|(\mathcal{C}_h P_h)^*(\mathcal{C}_h P_h)\|_{\mathcal{L}(V)} \\ & \leq \|P_h^*\|_{\mathcal{L}(V_h, V)} \|\mathcal{C}_h^*\|_{\mathcal{L}(Z, V_h)} \|\mathcal{C}_h\|_{\mathcal{L}(V_h, Z)} \|P_h\|_{\mathcal{L}(V, V_h)} \leq C. \end{aligned}$$

350 Similarly, $\|\mathcal{B}_h\|_{\mathcal{L}(U, V_h)} \leq \|\mathcal{B}\|_{\mathcal{L}(U, V)}$, and we have

$$351 \quad (11) \quad \begin{aligned} \|S_h\|_{\mathcal{L}(V)} & \leq \|\text{Id}_h\|_{\mathcal{L}(V_h, V)} \|\mathcal{B}_h\|_{\mathcal{L}(U, V_h)} \|\mathcal{R}^{-1}\|_{\mathcal{L}(U)} \|\mathcal{B}_h^*\|_{\mathcal{L}(V_h, U)} \|\text{Id}_h^*\|_{\mathcal{L}(V, V_h)} \\ & \leq C. \end{aligned}$$

352 As in the proof of [Theorem 4.5](#) we can write the difference $\tilde{X}(t) - \tilde{Y}(t)$ as a sum
353 of eight terms so that

$$354 \quad \|\tilde{X}(t) - \tilde{Y}(t)\|_{\mathcal{L}(V)} \leq \|R_1\|_{\mathcal{L}(V)} + \|R_2\|_{\mathcal{L}(V)} + \int_0^t \sum_{j=3}^8 \|R_j\|_{\mathcal{L}(V)} ds.$$

355

356 For R_1 we have

$$357 \quad \|R_1\|_{\mathcal{L}(V)} \leq \|E_h(t)^*\|_{\mathcal{L}(V)} \|\tilde{X}(0)\|_{\mathcal{L}(V)} \|E_h(t) - E_{\text{ms}}(t)\|_{\mathcal{L}(V)} \\ 358 \quad \leq CHt^{-1/2} \|X(0)\|_{\mathcal{L}(V)} \leq CHt^{-1/2},$$

360 and similarly we prove $\|R_2\|_{\mathcal{L}(V)} \leq CHt^{-1/2}$, where we have used that

$$361 \quad \|X_h(0)\|_{\mathcal{L}(V)} = \|\text{Id}_h^* X(0) \text{Id}_h\|_{\mathcal{L}(V)} \leq C \|X(0)\|_{\mathcal{L}(V)},$$

363 which is bounded due to [Assumption 4.8](#). Using the bounds (10) and (11) we get

$$364 \quad \int_0^t \sum_{j=3}^6 \|R_j\|_{\mathcal{L}(V)} \, ds \leq \int_0^t CH(t-s)^{-1/2} \, ds \leq CHt^{1/2}, \\ 365$$

366 and

$$367 \quad \int_0^t \|R_7\|_{\mathcal{L}(V)} + \|R_8\|_{\mathcal{L}(V)} \, ds \leq \int_0^t CH(t-s)^{-1/2} \|\tilde{X}(s) - \tilde{Y}(s)\|_{\mathcal{L}(V)} \, ds. \\ 368$$

369 By applying (generalized) Grönwall's lemma we obtain the desired error bound. \square

370 **5. Matrix-valued formulation.** To perform actual computations, we write the
371 finite-dimensional equations on matrix form by expressing the equations in the FEM
372 or LOD bases. To this end, let the function $x \in V_h$ and the operator $X_h: V_h \rightarrow V_h$
373 have the vector and matrix representations $\mathbf{x} \in \mathbb{R}^{N_h}$ and $\tilde{\mathbf{X}}^h \in \mathbb{R}^{N_h \times N_h}$, i.e.

$$374 \quad (12) \quad x = \sum_{j=1}^{N_h} \mathbf{x}_j \varphi_j^h \quad \text{and} \quad X_h x = \sum_{i,j=1}^{N_h} \tilde{\mathbf{X}}_{i,j}^h \mathbf{x}_j \varphi_i^h$$

375 Since exactly the same results hold for V_H upon replacing h by H , we frequently omit
376 the h sub- and superscripts in the following manipulations. They will be reinstated
377 later when we compare different discretizations. The coordinates satisfy

$$378 \quad \mathbf{M}\mathbf{x} = ((x, \varphi_i))_{i=1}^N \quad \text{and} \quad \mathbf{M}\tilde{\mathbf{X}} = ((X_h \varphi_j, \varphi_i))_{i,j=1}^N,$$

379 where \mathbf{M} denotes the (symmetric) mass matrix, $\mathbf{M}_{i,j} = (\varphi_j, \varphi_i)$. Unfortunately, we
380 will not recover the usual form of the matrix-valued DRE when working in these
381 coordinates. Therefore, we perform the change of variables

$$382 \quad \mathbf{X}\mathbf{M} = \tilde{\mathbf{X}}.$$

383 Coincidentally, this means that we actually have

$$384 \quad (13) \quad X_h x = \sum_{i,j=1}^N \mathbf{X}_{i,j} (x, \varphi_j) \varphi_i.$$

385 [Equation \(5\)](#) is equivalent to

$$386 \quad (14) \quad \left(\dot{X}_h \varphi_i, \varphi_j \right) = (X_h \varphi_i, \mathcal{A}_h \varphi_j) + (X_h \varphi_j, \mathcal{A}_h \varphi_i) \\ 387 \quad + (\mathcal{C}_h \varphi_i, \mathcal{C}_h \varphi_j)_Z - (\mathcal{R}^{-1} \mathcal{B}_h^* X_h \varphi_i, \mathcal{B}_h^* X_h \varphi_j)_U$$

389 for $1 \leq i, j \leq N$, and since $X_h \varphi_i = \sum_{k=1}^N (\mathbf{X}\mathbf{M})_{k,i} \varphi_k$, the first term becomes

$$390 \quad \sum_{k=1}^N (\dot{\mathbf{X}}\mathbf{M})_{k,i} \mathbf{M}_{j,k} = (\mathbf{M}\dot{\mathbf{X}}\mathbf{M})_{j,i}$$

391 Likewise, with the (negative) stiffness matrix $\mathbf{A}_{i,j} = (\mathcal{A}\varphi_j, \varphi_i)$, the second and third
392 terms become

$$393 \quad \sum_{k=1}^N (\mathbf{X}\mathbf{M})_{k,i} \mathbf{A}_{k,j} + \sum_{k=1}^N (\mathbf{X}\mathbf{M})_{k,j} \mathbf{A}_{k,i} = (\mathbf{A}^T \mathbf{X}\mathbf{M})_{j,i} + (\mathbf{M}\mathbf{X}\mathbf{A})_{j,i},$$

394 due to the symmetry of \mathbf{M} and \mathbf{X} . (Recall that we search for a self-adjoint operator
395 X_h .) Finally, the last two terms can be written

$$396 \quad (\mathbf{C}^T \mathbf{C})_{j,i} \quad \text{and} \quad (\mathbf{M}\mathbf{X}\mathbf{B}\mathbf{R}^{-1}\mathbf{B}^T \mathbf{X}\mathbf{M})_{j,i},$$

397 where $\mathbf{B}_{i,j} = (\mathcal{B}\varphi_j^U, \varphi_i)$, $\mathbf{R}_{i,j} = (\mathcal{R}\varphi_j^U, \varphi_i^U)$, $\mathbf{C}_{i,j} = (\mathcal{C}\varphi_j, \varphi_i^Z)$ and $\{\varphi_i^U\}$, $\{\varphi_i^Z\}$
398 denote orthonormal bases for U and Z , respectively. Summarizing, we can write the
399 equation on matrix form as

$$400 \quad (15) \quad \mathbf{M}\dot{\mathbf{X}}\mathbf{M} = \mathbf{M}\mathbf{X}\mathbf{A} + \mathbf{A}^T \mathbf{X}\mathbf{M} + \mathbf{C}^T \mathbf{C} - \mathbf{M}\mathbf{X}\mathbf{B}\mathbf{R}^{-1}\mathbf{B}^T \mathbf{X}\mathbf{M}.$$

401 Similar to the relations between the fine and coarse operators (6), it is easily
402 shown that their matrix representations satisfy

$$403 \quad \mathbf{A}_H = (\mathbf{I}_H^h)^T \mathbf{A}_h \mathbf{I}_H^h, \quad \mathbf{B}_H = (\mathbf{I}_H^h)^T \mathbf{B}_h, \quad \mathbf{C}_H = \mathbf{C}_h \mathbf{I}_H^h \quad \text{and} \quad \mathbf{M}_H = (\mathbf{I}_H^h)^T \mathbf{M}_h \mathbf{I}_H^h,$$

404 where $\mathbf{I}_H^h \in \mathbb{R}^{N_h \times N_H}$ is the prolongation matrix that satisfies $\mathbf{I}_H^h \mathbf{x}^H = \mathbf{x}^h$ if $x =$
405 $\sum_{j=1}^{N_H} \mathbf{x}_j^H \varphi_j^H$ and $\text{Id}_H^h x = \sum_{j=1}^{N_h} \mathbf{x}_j^h \varphi_j^h$. By expressing the φ^H functions in terms of
406 φ^h , it can be seen that $(\mathbf{I}_H^h)_{i,j} = \varphi_j^H(z_i)$, where z_i is the i :th node of \mathcal{T}_h . Thus the
407 coarse systems are easily constructed when the fine system is known. Note, however,
408 that the matrix representation of $(\text{Id}_H^h)^*$ is not $(\mathbf{I}_H^h)^T$ but $\mathbf{M}_H^{-1} (\mathbf{I}_H^h)^T \mathbf{M}_h$.

409 For the LOD case, we let \mathbf{Q}_h and $\mathbf{R}_h = \mathbf{I}_H^h - \mathbf{Q}_h$ be the matrix representations
410 of Q_h and R_h , respectively. To compute them efficiently, we follow [8]. Then

$$411 \quad X_H^{\text{ms}} x = \sum_{i=1}^{N_H} (\mathbf{X}_H^{\text{ms}} \mathbf{M}_{\text{ms}} \mathbf{x})_i \varphi_i^H,$$

412 where \mathbf{X}_H^{ms} is symmetric and satisfies

$$413 \quad \mathbf{M}_{\text{ms}} \dot{\mathbf{X}}_H^{\text{ms}} \mathbf{M}_{\text{ms}} = \mathbf{M}_{\text{ms}} \mathbf{X}_H^{\text{ms}} \mathbf{A}_{\text{ms}} + \mathbf{A}_{\text{ms}}^T \mathbf{X}_H^{\text{ms}} \mathbf{M}_{\text{ms}} \\ 414 \quad + \mathbf{C}_{\text{ms}}^T \mathbf{C}_{\text{ms}} - \mathbf{M}_{\text{ms}} \mathbf{X}_H^{\text{ms}} \mathbf{B}_{\text{ms}} \mathbf{R}^{-1} \mathbf{B}_{\text{ms}}^T \mathbf{X}_H^{\text{ms}} \mathbf{M}_{\text{ms}},$$

416 with the matrices

$$417 \quad \mathbf{A}_{\text{ms}} = \mathbf{R}_h^T \mathbf{A}_h \mathbf{R}_h, \quad \mathbf{B}_{\text{ms}} = \mathbf{R}_h^T \mathbf{B}_h, \quad \mathbf{C}_{\text{ms}} = \mathbf{C}_h \mathbf{R}_h \quad \text{and} \quad \mathbf{M}_{\text{ms}} = \mathbf{R}_h^T \mathbf{M}_h \mathbf{R}_h.$$

418 Finally, we note that if $u \in V_h$, $w \in V_H$ and $(\text{Id}_{\text{ms}}^h)^* u = R_h w$, then in coordi-
419 nates we have $\mathbf{w} = \mathbf{M}_{\text{ms}}^{-1} \mathbf{R}_h^T \mathbf{M}_h \mathbf{u}$. This means that the matrix representation of
420 $\text{Id}_{\text{ms}}^h X_h^{\text{ms}} (\text{Id}_{\text{ms}}^h)^*$ is $\mathbf{R}_h \mathbf{X}_H^{\text{ms}} \mathbf{R}_h^T \mathbf{M}_h$.

421 **5.1. Error computation.** We measure the quality of different approximations
 422 as the $\mathcal{L}(L^2)$ -normed distance to a reference approximation at the final time T . In
 423 order to find a matrix representation for this, we first observe that since $\|P_h x\| \leq \|x\|$,
 424 we have

$$425 \quad \|\text{Id}_h X_h P_h\|_{\mathcal{L}(L^2)} = \sup_{\substack{x \in H \\ x \neq 0}} \frac{\|X_h P_h x\|}{\|x\|} \leq \sup_{\substack{x \in H \\ x \neq 0}} \frac{\|X_h P_h x\|}{\|P_h x\|} = \sup_{\substack{x \in V_h \\ x \neq 0}} \frac{\|X_h x\|}{\|x\|}.$$

426 But $P_h x = x$ for $x \in V_h$, so since $V_h \subset L^2$ we also get

$$427 \quad \|\text{Id}_h X_h P_h\|_{\mathcal{L}(L^2)} \geq \sup_{\substack{x \in V_h \\ x \neq 0}} \frac{\|X_h P_h x\|}{\|x\|} = \sup_{\substack{x \in V_h \\ x \neq 0}} \frac{\|X_h x\|}{\|x\|}.$$

428 To compute the $\mathcal{L}(L^2)$ -norm it is thus enough to test with $x = \sum_{i=1}^{N_h} \mathbf{x}_i \varphi_i^h \in V_h$. Again
 429 omitting the h sub- and superscripts, we have that $(x, x) = \mathbf{x}^T \mathbf{M} \mathbf{x}$, and similarly

$$430 \quad (X_h x, X_h x) = \sum_{i,j,k,l=1}^N (\mathbf{X} \mathbf{M})_{i,j} \mathbf{x}_j (\mathbf{X} \mathbf{M})_{k,l} \mathbf{x}_l (\varphi_i, \varphi_k)$$

$$431 \quad = \mathbf{x}^T \mathbf{M}^T \mathbf{X}^T \mathbf{M} \mathbf{X} \mathbf{M} \mathbf{x}.$$

433 Since \mathbf{M} is symmetric positive definite, we may do a Cholesky factorization $\mathbf{M} =$
 434 $\mathbf{L}_M \mathbf{L}_M^T$, and the change of variables $\mathbf{y} = \mathbf{L}_M^T \mathbf{x}$ yields

$$435 \quad \|\text{Id}_h X_h P_h\|_{\mathcal{L}(L^2)} = \sup_{\substack{\mathbf{y} \in \mathbb{R}^N \\ \mathbf{y} \neq 0}} \frac{(\mathbf{y}^T \mathbf{L}_M^T \mathbf{X} \mathbf{L}_M \mathbf{L}_M^T \mathbf{X} \mathbf{L}_M \mathbf{y})^{1/2}}{(\mathbf{y}^T \mathbf{y})^{1/2}} = \|\mathbf{L}_M^T \mathbf{X} \mathbf{L}_M\|_{\mathbb{R}^{N \times N}},$$

436 where $\|\cdot\|_{\mathbb{R}^{N \times N}}$ denotes the standard spectral matrix norm. Recalling the matrix
 437 representation \mathbf{I}_H^h of Id_H^h , we now get that

$$438 \quad \|\text{Id}_h X_h P_h - \text{Id}_H X_H P_H\|_{\mathcal{L}(L^2)} = \|\mathbf{L}_M^T (\mathbf{X}_h - \mathbf{I}_H^h \mathbf{X}_H (\mathbf{I}_H^h)^T) \mathbf{L}_M\|_{\mathbb{R}^{N \times N}}.$$

439 The LOD error is completely analogous, using instead \mathbf{R}_h and \mathbf{X}_H^{ms} .

440 A similar approach also allows us to compute $\mathcal{L}(V)$ -errors. Let $\mathbf{A} = \mathbf{L}_A \mathbf{L}_A^T$ be a
 441 Cholesky factorization of \mathbf{A} . Then

$$442 \quad \|\text{Id}_h X_h P_h - \text{Id}_H X_H P_H\|_{\mathcal{L}(V)} \leq \|P_h\|_{\mathcal{L}(V, V_h)} \|\mathbf{L}_A^T (\mathbf{X}_h - \mathbf{I}_H^h \mathbf{X}_H (\mathbf{I}_H^h)^T) \mathbf{M} \mathbf{L}_A^{-T}\|_{\mathbb{R}^{N \times N}}.$$

443 We also get that $\|\text{Id}_h X_h P_h - \text{Id}_H X_H P_H\|_{\mathcal{L}(V)}$ is bounded from below by $\|\mathbf{L}_A^T (\mathbf{X}_h -$
 444 $\mathbf{I}_H^h \mathbf{X}_H (\mathbf{I}_H^h)^T) \mathbf{M} \mathbf{L}_A^{-T}\|_{\mathbb{R}^{N \times N}}$, i.e. the latter quantity can be thought of as an equivalent
 445 norm. Since \mathbf{L}_A is triangular, the extra cost required for the computation of \mathbf{L}_A^{-T}
 446 is negligible. If the low-rank formulation is used (see [subsection 6.1](#)), only a small
 447 number of linear equation systems involving \mathbf{L}_A needs to be solved, reducing the cost
 448 even further.

449 **6. Temporal discretization.** We discretize the matrix-valued DREs in time
 450 by means of a low-rank splitting scheme, since the basic operation in such methods
 451 is the application of $e^{t\mathbf{A}^T}$, i.e. essentially solving a parabolic problem. Let τ denote
 452 a fixed time step, and let $t_j = j\tau$, $j = 1, \dots, N_t$, be the time discretization of the

453 interval $[0, T]$. We split Equation (15) into two parts, $\dot{\mathbf{X}} = \mathcal{F}\mathbf{X} + \mathcal{G}\mathbf{X}$, where

454
$$\mathcal{F}\mathbf{X} = \mathbf{X}\mathbf{A}\mathbf{M}^{-1} + \mathbf{M}^{-1}\mathbf{A}^T\mathbf{X} + \mathbf{M}^{-1}\mathbf{C}^T\mathbf{C}\mathbf{M}^{-1} \quad \text{and} \quad \mathcal{G}\mathbf{X} = -\mathbf{X}\mathbf{B}\mathbf{R}^{-1}\mathbf{B}^T\mathbf{X}.$$

455 Then the Strang splitting approximation at time t_j is given by \mathbf{X}^j , with $\mathbf{X}^0 = \mathbf{X}(0)$
456 and

457
$$\mathbf{X}^{j+1} = e^{\frac{\tau}{2}\mathcal{F}} e^{\tau\mathcal{G}} e^{\frac{\tau}{2}\mathcal{F}} \mathbf{X}^j.$$

458 Here, the solution operators $e^{t\mathcal{F}}$ and $e^{t\mathcal{G}}$ satisfy

459 (16)
$$e^{t\mathcal{F}}\mathbf{X} = e^{t\mathbf{M}^{-T}\mathbf{A}^T}\mathbf{X}e^{t\mathbf{A}\mathbf{M}^{-1}} + \int_0^t e^{s\mathbf{M}^{-T}\mathbf{A}^T}\mathbf{M}^{-T}\mathbf{C}^T\mathbf{C}\mathbf{M}^{-1}e^{s\mathbf{A}\mathbf{M}^{-1}} ds,$$

460 (17)
$$e^{t\mathcal{G}}\mathbf{X} = (\mathbf{I} + t\mathbf{X}\mathbf{B}\mathbf{R}^{-1}\mathbf{B}^T)^{-1}\mathbf{X},$$

462 where the first equality is apparent from the integral formulation (9), while the second
463 is easily verified by differentiation.

464 The low-rank version of the method relies on the assumption that the solution \mathbf{X}
465 has low rank. This is general true for LQR problems and dramatically reduces the
466 computational cost. In that case, we may factorize $\mathbf{X} = \mathbf{L}\mathbf{D}\mathbf{L}^T$, where $\mathbf{L} \in \mathbb{R}^{N_h \times r}$
467 and $\mathbf{D} \in \mathbb{R}^{r \times r}$ with the rank $r \ll N_h$. Also $e^{\tau\mathcal{F}}\mathbf{X}$ and $e^{\tau\mathcal{G}}\mathbf{X}$, and thus the iterates \mathbf{X}_j ,
468 may then be factorized in such a way. After a reformulation, $e^{\tau\mathcal{G}}\mathbf{X}$ is very cheap to
469 compute, and the computation of $e^{\tau\mathcal{F}}\mathbf{X}$ reduces to an evaluation of $e^{\tau\mathbf{M}^{-T}\mathbf{A}^T}\mathbf{L}$ (plus
470 preliminary, similar work for the integral term). The latter operation is equivalent to
471 solving $\mathbf{M}\dot{x} = \mathbf{A}^T x$, $x(0) = \mathbf{L}$, and the matrix \mathbf{M} is thus never explicitly inverted.
472 For further details, we refer to [18, 19].

473 **6.1. Low-rank errors.** Also the error computations outlined in subsection 5.1
474 benefit from being formulated in a low-rank setting. Assume that $\mathbf{X}_h = \mathbf{L}_h\mathbf{D}_h\mathbf{L}_h^T$
475 and $\mathbf{X}_H = \mathbf{L}_H\mathbf{D}_H\mathbf{L}_H^T$ with $\mathbf{L}_h \in \mathbb{R}^{N_h \times r_h}$ and $\mathbf{L}_H \in \mathbb{R}^{N_H \times r_H}$ with $r_h, r_H \ll N_h$, and
476 let $\mathbf{M}_h = \mathbf{L}_M\mathbf{L}_M^T$ be a Cholesky factorization. By setting

477
$$\mathbf{V} = [\mathbf{L}_M^T\mathbf{L}_h \quad \mathbf{L}_M^T\mathbf{I}_H^h\mathbf{L}_H] \quad \text{and} \quad \mathbf{D} = \begin{bmatrix} \mathbf{D}_h & 0 \\ 0 & -\mathbf{D}_H \end{bmatrix}$$

478 we see that $\mathbf{V} \in \mathbb{R}^{N_h \times (r_h + r_H)}$, $\mathbf{D} \in \mathbb{R}^{(r_h + r_H) \times (r_h + r_H)}$ and it follows that

479
$$\mathbf{L}_M^T(\mathbf{X}_h - \mathbf{I}_H^h\mathbf{X}_H(\mathbf{I}_H^h)^T)\mathbf{L}_M = \mathbf{V}\mathbf{D}\mathbf{V}^T.$$

480 Since $\mathbf{V}\mathbf{D}\mathbf{V}^T$ is not necessarily an eigenvalue decomposition, we cannot immediately
481 determine the norm by inspection. However, performing a QR-factorization $\mathbf{V} = \mathbf{Q}\mathbf{R}$
482 is cheap if the number of columns is low, and $\mathbf{R}\mathbf{D}\mathbf{R}^T \in \mathbb{R}^{(r_h + r_H) \times (r_h + r_H)}$ can also
483 be diagonalized cheaply. (This is precisely the LDL^T column compression procedure
484 which is applied in each time step.) We acquire $\mathbf{V}\mathbf{D}\mathbf{V}^T = (\mathbf{Q}\mathbf{W})\tilde{\mathbf{D}}(\mathbf{Q}\mathbf{W})^T$, for some
485 \mathbf{W} , where $\|\mathbf{V}\mathbf{D}\mathbf{V}^T\| = |\tilde{\mathbf{D}}_{1,1}|$.

486 For errors in the $\mathcal{L}(\mathbf{V})$ -norm, we do not get a symmetric matrix as above. But if
487 $\mathbf{A} = \mathbf{L}_A\mathbf{L}_A^T$ we can still write

488
$$\mathbf{L}_A^T(\mathbf{X}_h - \mathbf{I}_H^h\mathbf{X}_H(\mathbf{I}_H^h)^T)\mathbf{M}\mathbf{L}_A^{-T} = \mathbf{G}_1\mathbf{D}\mathbf{G}_2^T,$$

489 with the same \mathbf{D} , and with

490
$$\mathbf{G}_1 = [\mathbf{L}_A^T\mathbf{L}_h \quad \mathbf{L}_A^T\mathbf{I}_H^h\mathbf{L}_H] \quad \text{and} \quad \mathbf{G}_2 = [\mathbf{L}_A^{-1}\mathbf{M}\mathbf{L}_h \quad \mathbf{L}_A^{-1}\mathbf{M}\mathbf{I}_H^h\mathbf{L}_H].$$

491 We can cheaply QR -factorize both $\mathbf{G}_1 = \mathbf{U}\mathbf{R}_1$ and $\mathbf{G}_2 = \mathbf{V}\mathbf{R}_2$; this means that

$$492 \quad \|\mathbf{L}_A^T(\mathbf{X}_h - \mathbf{I}_H^h \mathbf{X}_H (\mathbf{I}_H^h)^T) \mathbf{M} \mathbf{L}_A^{-T}\|_{\mathbb{R}^{N_h \times N_h}} = \|\mathbf{U} \mathbf{S} \mathbf{V}^T\|_{\mathbb{R}^{N_h \times N_h}} = \|\mathbf{S}\|_{\mathbb{R}^{N_h \times N_h}},$$

493 where $\mathbf{S} = \mathbf{R}_1 \mathbf{D} \mathbf{R}_2^T$ is a small matrix.

494 **7. Numerical experiments.** We have performed a number of numerical exper-
495 iments in order to verify our a priori error bounds for the LOD discretizations, and
496 to demonstrate their efficiency in comparison to the classical FEM.

497 In all experiments, we compute the relevant matrices for both FEM and LOD
498 by using efficient code by Fredrik Hellman and Daniel Elfverson¹. These pre-solve
499 computations were run on a Intel[®] Core[™] i7-5600U processor. We note that the
500 localized elliptic fine-scale problems were not solved in parallel. Doing so would further
501 improve the performance of LOD.

502 For approximating the solutions to the DREs, we employ in all cases the low-rank
503 Strang splitting scheme (as described in [section 6](#)) with $N_t = 256$ time steps. This
504 ensures that the temporal error is small compared to the spatial error, which is our
505 interest here. Our implementation utilizes the DREsplit² library. These computations
506 were run on the C3SE cluster, each using a single Intel[®] Xeon[®] E5-2650 v3 processor.

507 **7.1. Example 1.** In this first example, we consider diffusion on the unit square.
508 More specifically, we take $\Omega = [0, 1]^2$ and set $\mathcal{A}u = \nabla \cdot (\kappa \nabla u)$ with Dirichlet boundary
509 conditions. Here, κ is piecewise constant on a square grid of size 2^{-6} and taking
510 randomly chosen values in $[0.1, 100]$. We consider 3 independent inputs and define
511 the input operator \mathcal{B} as the sum

$$512 \quad \mathcal{B}u = \sum_{j=1}^3 \mathcal{B}_j u_j, \quad \text{where} \quad (\mathcal{B}_j u)(x, y) = \begin{cases} 1, & \frac{j}{4} \leq x, y \leq \frac{j}{4} + \frac{1}{8}. \\ 0, & \text{otherwise} \end{cases}.$$

513 Thus we can control the system on three small squares. As the output operator we
514 take the mean, i.e. $\mathcal{C}x = \int_{\Omega} x$.

515 For the discretization in space, we start with a coarse mesh containing 8 triangles,
516 and then refine this 5 times, giving meshes with 2^{3+2j} triangles, for $j = 0, \dots, 5$. One
517 additional refinement provides the reference grid with $2^{13} = 32768$ triangles. This
518 results in matrices $\mathbf{A}_j \in \mathbb{R}^{n \times n}$, $\mathbf{B}_j \in \mathbb{R}^{n \times 3}$ and $\mathbf{C}_j \in \mathbb{R}^{1 \times n}$, $j = 0, \dots, 6$, with
519 $n = 1, 9, 49, 225, 961, 3969, 16129$ (since we only consider the interior nodes).

520 The approximations are compared only at the final time, in the $\mathcal{L}(L^2)$ - and $\mathcal{L}(V)$ -
521 norms as outlined in [subsection 5.1](#), and the computed errors are shown in [Figure 1](#).
522 We see that the classical FEM initially struggles due to not resolving the multiscale
523 coefficient properly, but converges with order 2 when the mesh becomes fine enough.
524 The LOD approach converges with order 2 also for the coarse meshes, and additionally
525 results in approximations that are about one order of magnitude more accurate. The
526 plot to the right shows the errors against the actual computation time, including the
527 time spent on constructing the LOD bases. As can be seen, this extra effort is low
528 enough that except for the most inaccurate cases it is always worthwhile to use the
529 LOD approach.

¹Available on request from Fredrik Hellman, fredrik.hellman@it.uu.se.

²Available on request from Tony Stillfjord, tony.stillfjord@gu.se, or <http://www.chalmers.se/en/Staff/Pages/tonyst.aspx>.

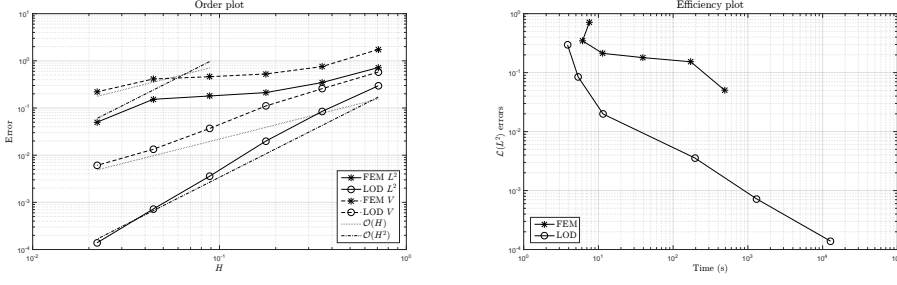


FIG. 1. Left: The $\mathcal{L}(L^2)$ - and $\mathcal{L}(V)$ -norm errors of the approximations computed in [Example 1](#), plotted against the meshwidth. Right: The $\mathcal{L}(L^2)$ -norm errors plotted against the computation time.

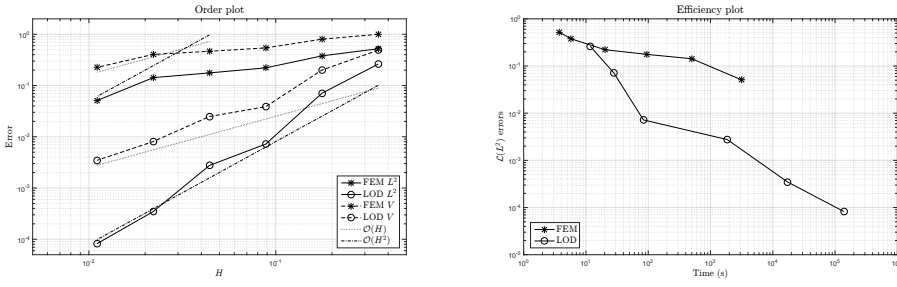


FIG. 2. Left: The $\mathcal{L}(L^2)$ - and $\mathcal{L}(V)$ -norm errors of the approximations computed in [Example 2](#), plotted against the meshwidth. Right: The $\mathcal{L}(L^2)$ -norm errors plotted against the computation time.

530 **7.2. Example 2.** Here, we consider an L-shaped domain Ω , where $[0.5, 1] \times$
 531 $[0.5, 0.5]$ has been removed from the unit square. The diffusion coefficient κ is piece-
 532 wise constant on a square grid of size 2^{-6} and taking random values in $[0.1, 100]$. We
 533 use one control input, given by the characteristic function of the square $[0.65, 0.85]^2$,
 534 and one output, the mean over the square $[0.15, 0.35]^2$. The meshes are setup as
 535 in the previous example, but now with $n = 5, 33, 161, 705, 2945, 12033$ interior nodes
 536 ($n = 48641$ for the reference solution). The time discretization is the same as in the
 537 previous example.

538 The results are shown in [Figure 2](#). Due to the reentrant corner the errors behave
 539 more erratically than in the previous example, but LOD is still clearly first- and
 540 second-order convergent in contrast to standard FEM, which performs very poorly.
 541 We also observe that LOD is more efficient in all but the coarsest cases.

542 **7.3. Example 3.** We again consider the setting of [Example 1](#), but replace the
 543 diffusivity constant. Here, κ takes the constant value 10 everywhere, except for in 7
 544 horizontal stripes where it is 0.1. The stripes are centered around the heights $j/8$,
 545 $j = 1, \dots, 7$, and have a width of 2^{-6} .

546 The results are shown in [Figure 3](#). This time, the detrimental effect on the FEM
 547 discretization is even more pronounced, with almost no convergence until the thin
 548 stripes can be resolved. The LOD approximations are once again more accurate for
 549 all H . We note that the $\mathcal{L}(L^2)$ -error is not quite $\mathcal{O}(H^2)$ in this case, but rather
 550 close to $\mathcal{O}(H^2 \log H^{-1})$ as predicted by [Theorem 4.5](#). Like in the previous example,
 551 computing the LOD bases is cheap enough that the LOD approach is more efficient
 552 in all but the least accurate cases.

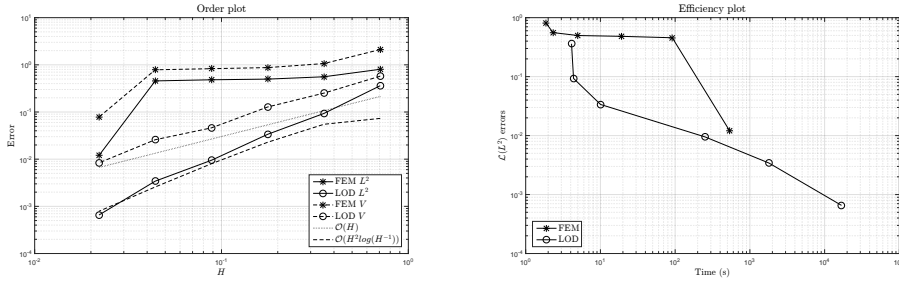


FIG. 3. Left: The $\mathcal{L}(L^2)$ - and $\mathcal{L}(V)$ -norm errors of the approximations computed in *Example 3*, plotted against the meshwidth. Right: The $\mathcal{L}(L^2)$ -norm errors plotted against the computation time.

553 **7.4. Example 4.** In this example, we deviate from the basic setting described in
 554 *section 4* by considering a boundary control application. All parameters except for the
 555 boundary conditions and the input operator are the same as in *Example 1*. We call
 556 the union of the top and bottom edges of the unit square Γ_D and impose homogeneous
 557 Dirichlet boundary conditions there. The left and right edges we denote Γ_1 and Γ_2 ,
 558 respectively, and there we impose nonhomogeneous Neumann boundary conditions.
 559 In particular, with the outward-pointing normal denoted by n , we consider functions
 560 x satisfying

$$561 \quad \kappa \nabla x \cdot n = \Psi u_i \quad \text{on } \Gamma_i.$$

562 Here, u_1 and u_2 are the two control inputs, and

$$563 \quad \Psi: s \mapsto \begin{cases} 2s, & 0 \leq s \leq 1/2, \\ 2(1-s), & 1/2 < s \leq 1, \end{cases}$$

564 is a fixed function. The operator \mathcal{A} now corresponds to $x \mapsto \nabla \cdot (\kappa \nabla x)$ on $H_{\Gamma_D}^1(\Omega)$
 565 with no conditions imposed on Γ_1, Γ_2 , while the (unbounded) operator \mathcal{B} implements
 566 the boundary conditions. We refrain from elaborating further on this here, and simply
 567 note that the FEM matrix representation becomes

$$568 \quad \mathbf{B}_{j,i}^h = \int_{\Gamma_i} \Psi \varphi_j^h.$$

569 For further details on the proper abstract framework, see e.g. [12].

570 Since *Assumption 2.1* is no longer satisfied, we may not apply *Theorem 4.5*. How-
 571 ever, the results plotted in *Figure 4* are similar to the results in previous examples.
 572 Again, the LOD approximations are more efficient except for the very coarsest meshes.
 573 This indicates that our theory could be extended also to the case of unbounded oper-
 574 ators \mathcal{B} and \mathcal{C} .

575 **Acknowledgments.** We are grateful to Fredrik Hellman for his assistance with
 576 the code for computing the LOD bases.

577

REFERENCES

- 578 [1] H. ABOU-KANDIL, G. FREILING, V. IONESCU, AND G. JANK, *Matrix Riccati equations*, Systems
 579 & Control: Foundations & Applications, Birkhäuser, Basel, 2003, [https://doi.org/10.1007/](https://doi.org/10.1007/978-3-0348-8081-7)
 580 [978-3-0348-8081-7](https://doi.org/10.1007/978-3-0348-8081-7).

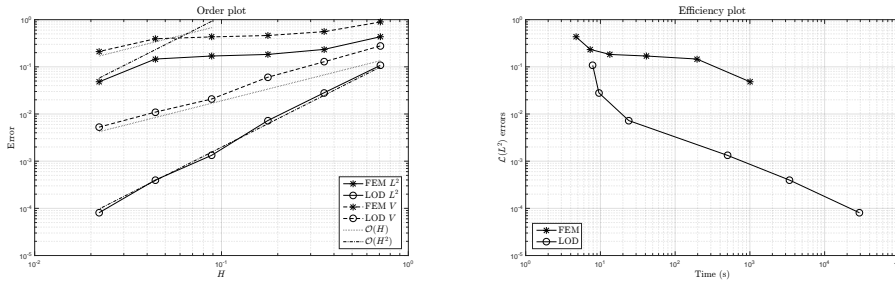


FIG. 4. Left: The L^2 - and $L(V)$ -norm errors of the approximations computed in Example 4, plotted against the meshwidth. Right: The L^2 -norm errors plotted against the computation time.

- 581 [2] R. E. BANK AND H. YSERENTANT, *On the H^1 -stability of the L_2 -projection onto finite*
582 *element spaces*, Numer. Math., 126 (2014), pp. 361–381, [https://doi.org/10.1007/](https://doi.org/10.1007/s00211-013-0562-4)
583 [s00211-013-0562-4](https://doi.org/10.1007/s00211-013-0562-4).
- 584 [3] P. BENNER AND H. MENA, *Numerical solution of the infinite-dimensional LQR problem and*
585 *the associated Riccati differential equations*, J. Numer. Math., (2016), [https://doi.org/10.](https://doi.org/10.1515/jnma-2016-1039)
586 [1515/jnma-2016-1039](https://doi.org/10.1515/jnma-2016-1039). Advance online publication, retrieved 23 Nov. 2016.
- 587 [4] A. BENSOUSSAN, G. DA PRATO, M. C. DELFOUR, AND S. K. MITTER, *Representation and*
588 *control of infinite dimensional systems*, Systems & Control: Foundations & Applications,
589 Birkhäuser Boston, Inc., Boston, MA, second ed., 2007, [https://doi.org/10.1007/](https://doi.org/10.1007/978-0-8176-4581-6)
590 [978-0-8176-4581-6](https://doi.org/10.1007/978-0-8176-4581-6).
- 591 [5] W. E. BOSARGE, JR., O. G. JOHNSON, AND C. L. SMITH, *A direct method approximation to the*
592 *linear parabolic regulator problem over multivariate spline bases*, SIAM J. Numer. Anal.,
593 10 (1973), pp. 35–49, <https://doi.org/10.1137/0710006>.
- 594 [6] L. CAO, J. LIU, W. ALLEGRETTO, AND Y. LIN, *A multiscale approach for optimal control*
595 *problems of linear parabolic equations*, SIAM J. Control Optim., 50 (2012), pp. 3269–3291,
596 <https://doi.org/10.1137/110828800>.
- 597 [7] Y. CHEN, Y. HUANG, W. LIU, AND N. YAN, *A mixed multiscale finite element method for*
598 *convex optimal control problems with oscillating coefficients*, Comput. Math. Appl., 70
599 (2015), pp. 297–313, <https://doi.org/10.1016/j.camwa.2015.03.020>.
- 600 [8] C. ENGWER, P. HENNING, A. MÅLQVIST, AND D. PETERSEIM, *Efficient implementation of the*
601 *Localized Orthogonal Decomposition method*, ArXiv e-prints, (2016), [https://arxiv.org/](https://arxiv.org/abs/1602.01658)
602 [abs/1602.01658](https://arxiv.org/abs/1602.01658). <https://arxiv.org/abs/1602.01658>.
- 603 [9] R. S. FALK, *Approximation of a class of optimal control problems with order of convergence*
604 *estimates*, J. Math. Anal. Appl., 44 (1973), pp. 28–47, [https://doi.org/10.1016/0022-247X\(73\)](https://doi.org/10.1016/0022-247X(73)90022-X)
605 [90022-X](https://doi.org/10.1016/0022-247X(73)90022-X).
- 606 [10] P. HENNING AND A. MÅLQVIST, *Localized orthogonal decomposition techniques for boundary*
607 *value problems*, SIAM J. Sci. Comput., 36 (2014), pp. A1609–A1634, [https://doi.org/10.](https://doi.org/10.1137/130933198)
608 [1137/130933198](https://doi.org/10.1137/130933198).
- 609 [11] M. KROLLER AND K. KUNISCH, *Convergence rates for the feedback operators arising in the linear*
610 *quadratic regulator problem governed by parabolic equations*, SIAM J. Numer. Anal., 28
611 (1991), pp. 1350–1385, <https://doi.org/10.1137/0728071>.
- 612 [12] I. LASIECKA AND R. TRIGGIANI, *Control theory for partial differential equations: continuous*
613 *and approximation theories. I*, vol. 74 of Encyclopedia of Mathematics and its Applications,
614 Cambridge University Press, Cambridge, 2000. Abstract parabolic systems.
- 615 [13] J. LI, *A multiscale finite element method for optimal control problems governed by the elliptic*
616 *homogenization equations*, Comput. Math. Appl., 60 (2010), pp. 390–398, [https://doi.org/](https://doi.org/10.1016/j.camwa.2010.04.017)
617 [10.1016/j.camwa.2010.04.017](https://doi.org/10.1016/j.camwa.2010.04.017).
- 618 [14] A. MÅLQVIST AND A. PERSSON, *Multiscale techniques for parabolic equations*, ArXiv e-prints,
619 (2015), <https://arxiv.org/abs/1504.08140>. <https://arxiv.org/abs/1504.08140>.
- 620 [15] A. MÅLQVIST AND D. PETERSEIM, *Localization of elliptic multiscale problems*, Math. Comp.,
621 83 (2014), pp. 2583–2603.
- 622 [16] R. S. MCKNIGHT AND W. E. BOSARGE, JR., *The Ritz-Galerkin procedure for parabolic control*
623 *problems*, SIAM J. Control Optim., 11 (1973), pp. 510–524.
- 624 [17] I. G. ROSEN, *Convergence of Galerkin approximations for operator Riccati equations—a*
625 *nonlinear evolution equation approach*, J. Math. Anal. Appl., 155 (1991), pp. 226–248,
626 [https://doi.org/10.1016/0022-247X\(91\)90035-X](https://doi.org/10.1016/0022-247X(91)90035-X).

- 627 [18] T. STILLFJORD, *Low-rank second-order splitting of large-scale differential Riccati equations*,
628 IEEE Trans. Automat. Control, 60 (2015), pp. 2791–2796, [https://doi.org/10.1109/TAC.](https://doi.org/10.1109/TAC.2015.2398889)
629 [2015.2398889](https://doi.org/10.1109/TAC.2015.2398889).
- 630 [19] T. STILLFJORD, *Adaptive high-order splitting schemes for large-scale differential*
631 *Riccati equations*, ArXiv e-prints, (2016), <https://arxiv.org/abs/1612.00677>.
632 <https://arxiv.org/abs/1612.00677>.
- 633 [20] H. TANABE, *Equations of evolution*, vol. 6 of Monographs and Studies in Mathematics, Pit-
634 man (Advanced Publishing Program), Boston, Mass.-London, 1979. Translated from the
635 Japanese by N. Mugibayashi and H. Haneda.
- 636 [21] V. THOMÉE, *Galerkin Finite Element Methods for Parabolic Problems*, Springer Series in Com-
637 putational Mathematics, Springer-Verlag, Berlin, second ed., 2006.
- 638 [22] R. WINTHER, *Error estimates for a Galerkin approximation of a parabolic control problem*,
639 Ann. Mat. Pura Appl. (4), 117 (1978), pp. 173–206, <https://doi.org/10.1007/BF02417890>.